Investigation of strain accumulation along Tuzla fault – western Turkey

Emre HAVAZLI* ⓘ **, Haluk ÖZENER** ⓘ
Department of Geodesy, Kandilli Observatory and Earthquake Research Institute (KOERI), Boğaziçi University, İstanbul, Turkey

Abstract: The Aegean region is one of the most seismically active regions in Turkey and comprises the Hellenic Arc, Greece, and Western Turkey. The Tuzla Fault, which lies between the town of Menderes and Cape Doğanbey, is one of the major seismic threats in western Turkey due to its seismic potential to generate a major earthquake (M 6, near Doğanbey Cape in 1992) and proximity to the city of İzmir which sustained damage due to the earthquake that occurred in the Aegean Sea on October 30th, 2020. In order to estimate strain rates and seismic potential around the Tuzla Fault, five global positioning system (GPS) surveys were carried out between 2009 and 2012. Estimated GPS velocities in the study area exceed 20 mm/year, which is in line with previous studies. We use two different approaches to calculate the strain accumulation on and around the Tuzla Fault. The first method adopts forming triangles using the GPS sites as corners and calculating strain rates within those triangles. The second method adopts a bicubic interpolation approach described by Holt and Haines, 1993. Maximum values of strain accumulation were found to reach up to 200 nanostrain/year.

Key words: Tuzla Fault-İzmir, Aegean tectonics, strain rate, global positioning system GPS, velocity field

1. Introduction

The Aegean Region is located within the convergent boundary between the African and Eurasian plates. Since the late Miocene, the Aegean region has been under extension due to rollback of the subducting Nubian lithosphere (Reilinger and McClusky, 2011). Present-day extension across the Aegean region, as determined by GPS, exceeds 30 mm/year making it one of the most actively deforming continental regions on earth (McClusky et al.,2000). As a result, a group of E-W trending grabens have been developing in western Turkey (McKenzie, 1972; Şengör and Yilmaz, 1981; Mercier et al., 1989; Paton, 1992; Ergun and Oral, 2000; Yılmaz et al., 2000; Koçyiğit et al., 2000). These grabens are bounded by E-W trending normal fault zones which extend to about 100-150 km. These fault zones are generally segmented and each segment is no longer than 8-10 km (Yılmaz et al., 2000).

The distribution of earthquakes indicates that the Aegean Region is under north-south extension (Figure 1) (Saunders et al., 1998; Sodoudi et al., 2006). Earlier GPS studies quantify N-S extension at longitude 27°E to exceed 20 mm/year which is comparable to the 20–25 mm/year shear across the North Anatolian fault (McClusky et al., 2000, Aktug et al., 2009). Even though the previous studies report an extensive investigation and estimation of deformation characteristics of the Aegean region, they can't provide an estimation of deformation characteristics

for individual faults. It is important to study individual faults and estimate their deformation characteristics to be able to resolve complex deformation patterns in the region.

Our study focuses on the Tuzla Fault in the region, which is located within the extensional region. We studied the Tuzla Fault because of its proximity to the highly populated city of İzmir, Turkey, which suffered damage due to earthquake in the Aegean Sea on October 30th, 2020. Historical evidence and seismological observations indicate that the Tuzla Fault has the potential to generate large earthquakes that can reach up to M > 6 (Ilhan et al. 2004; Radius 1997).

Our study builds upon previous studies that has been carried out specifically on the Tuzla Fault. Geodetic investigation of the Tuzla Fault began in 2009 with the establishment of a micro geodetic network that includes 16 campaign sites on and around the fault (Halicioglu and Ozener, 2008). Five global positioning system (GPS) campaigns were carried out between 2009 and 2012, and the results were used to determine the horizontal velocity field (Ozener et al., 2013). In this study, we estimate the strain rates on and around the Tuzla Fault using GPS velocities estimated from five campaign measurements between 2009 and 2012.

Strain rate is determined by two different methods. The first method adopts a triangulation approach which uses GPS stations as corners of each triangle and estimates the
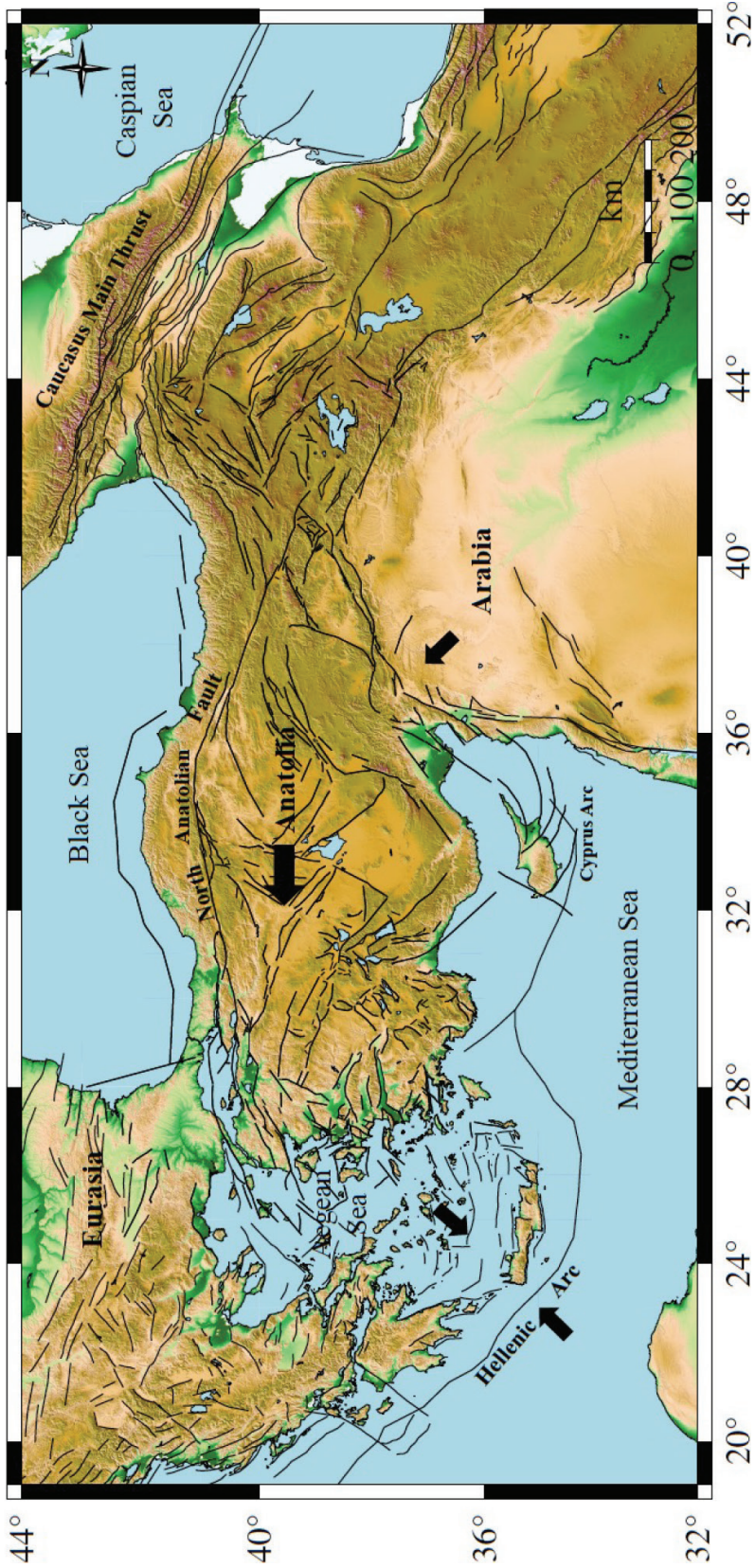
---

* Correspondence: emre.havazli@gmail.com

Figure 1. Kinematics of the Aegean Region and surrounding plates (adapted from Taymaz et al., 2007). Black lines represent active fault lines in the area (Danciu et al., 2018).

strain rates at the centers of triangles. The second method uses the interpolation of velocities over a regular grid method, described by Haines and Holt, (1993), and uses that information to estimate strain rates.

2. Seismicity and tectonics

Focal mechanisms for earthquakes indicate that faulting in the western part of the Aegean region of Turkey is mostly extensional in line with the nature of normal faults, with a NE to SW strike and slip vectors directed NW to N (Taymaz, 2001). The Tuzla Fault is located ~40 km southwest of İzmir and strikes NE-SW (Emre and Barka, 2000). It has a variety of names in literature, such as the Cumaovasi Fault, the Cumali Reverse Fault and the Orhanli Fault (Saroglu et al., 1987; Saroglu et al., 1992; Esder, 1988; Genç et al., 2001). The fault is 42 km long on land and continues in a SW direction another 10 km under the Aegean Sea.

The Tuzla Fault has 3 segments, the Catalca, Orhanli, and Cumali segments. The Catalca segment is the northeast part of the fault and is 15 km long striking N35E. The Catalca segment is a right-lateral strike-slip fault as estimated from quaternary geomorphologic data (Ozener et al., 2012; Sabuncu and Ozener, 2014). The Orhanli segment strikes N50E and is 16 km long and is the southeast segment of the Tuzla Fault. The Cumali segment is the largest fault segment and is composed of a number of sub-parallel branches striking NNE-SSW. It is 15 km long and continues in the Aegean Sea for 25 km more (Ocakoglu et al., 2005). A Mw = 6.0 earthquake occurred at the southern end of the Tuzla fault in 1992 near Doganbey Cape (Figure 2). Even though the morphology of the Doganbey Cape has been interpreted as a result of a left lateral slip, the focal mechanism solution indicates right lateral slip on the Tuzla Fault (Tan and Taymaz, 2001).

3. Data collection, processing, and analysis

GPS sites were established at distances of 1, 2, and 6 km from the fault trace. All sites were set into bedrock using high quality geodetic monuments (Figure 3). Table 1 gives the coordinates of GPS sites established in the study area.

Five GPS surveys were carried out in the study area between 2009 and 2012. Observation strategy was 10 h/day for 2 consecutive days at each site with 10-degree
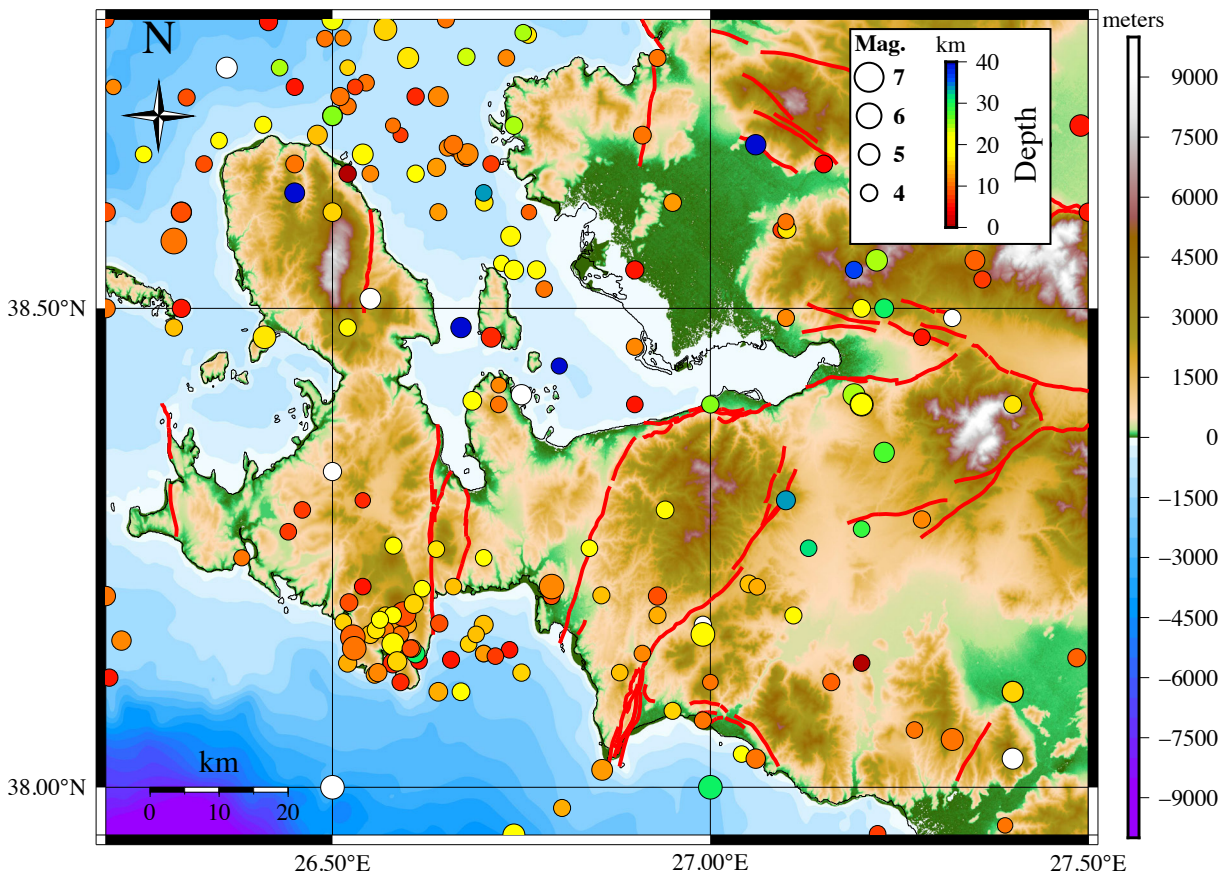
Figure 2. Seismicity of the study area between 1900 and December 2020 (KOERI Database). The circles represent Mw ≥ 4 earthquakes occurred over the study area. Size of each circle represents the magnitude of the respective earthquake while the color represents the depth. We can see that majority of the earthquakes in the area occur at depths of 20 km or less.
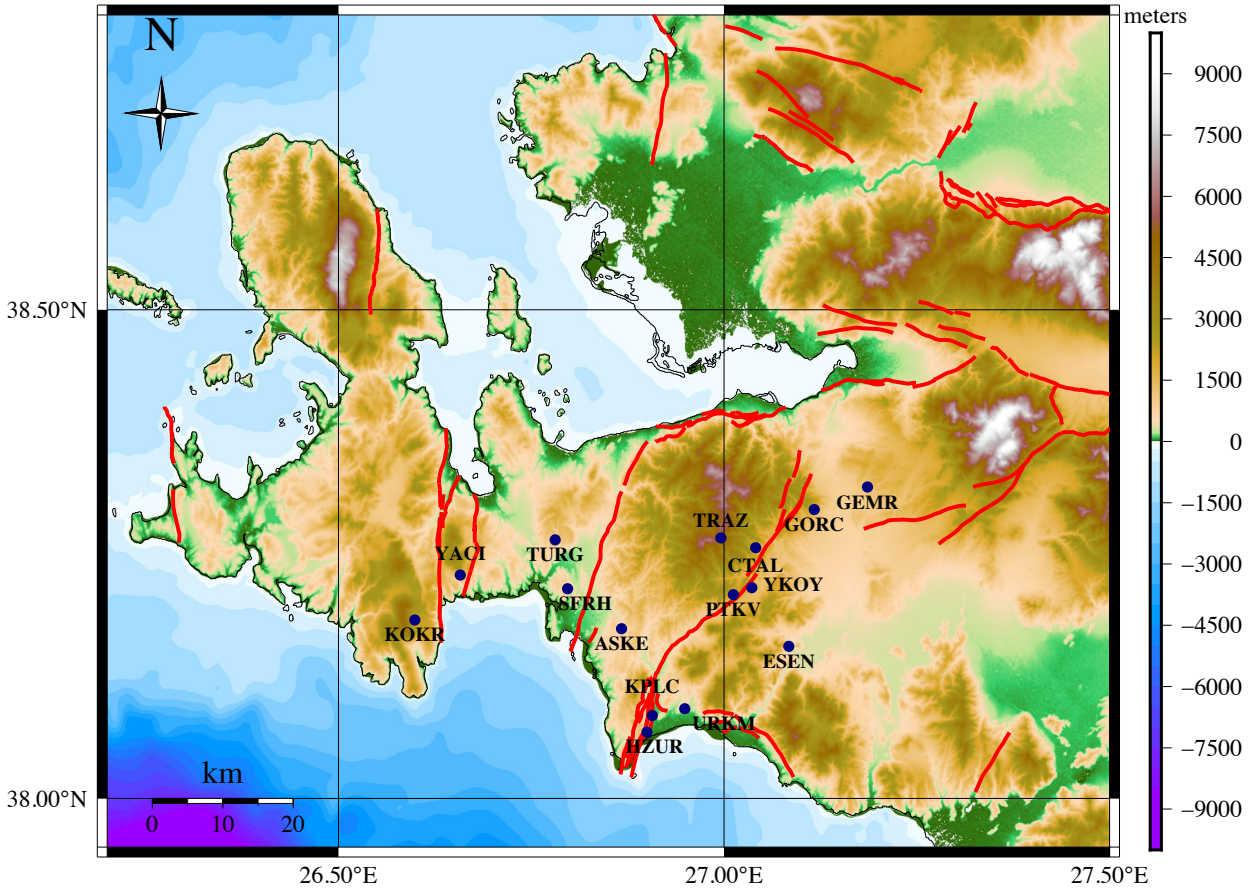
Figure 3. Locations of the GPS campaign sites established in the study area. See Table 1 for more details.

Table 1. GPS station locations along with their estimated velocity and their 95% confidence limit uncertainties.

Site	Latitude (deg)	Longitude (deg)	E_{vel} (mm/year)	N_{vel} (mm/year)	(mm/year)	(mm/year)	RHO
GEMR	38.31893	27.18589	−20.32	−16.69	1.45	1.30	0.031
GORC	38.29572	27.11659	−18.43	−18.16	1.33	1.19	0.005
ESEN	38.15567	27.08366	−19.44	−15.88	1.22	1.11	−0.044
CTAL	38.25710	27.04138	−19.89	−18.20	1.90	1.70	−0.014
YKOY	38.21573	27.03605	−19.32	−20.11	1.42	1.32	−0.084
PTKV	38.20897	27.01246	−20.75	−18.05	1.62	1.48	−0.006
TRAZ	38.26691	26.99559	−20.00	−17.00	1.52	1.35	0.010
URKM	38.09247	26.94867	−19.23	−20.03	1.36	1.22	0.008
KPLC	38.08517	26.90745	−18.50	−20.94	1.51	1.31	−0.004
HZUR	38.06769	26.90042	−18.58	−21.67	1.40	1.27	0.016
ASKE	38.17417	26.86663	−19.45	−17.66	1.43	1.29	−0.008
SFRH	38.21542	26.79729	−17.31	−18.15	1.46	1.36	0.013
TURG	38.26488	26.78140	−18.88	−20.83	1.47	1.32	−0.031
YACI	38.22923	26.65781	−19.18	−18.46	1.38	1.22	0.027
KOKR	38.18291	26.59937	−18.45	−21.17	1.51	1.38	0.007

elevation mask and 15 s data rate. In all campaigns some stations were observed both days to increase repeatability for the enhancement of repeatability.

The GAMIT/GLOBK (Herring et al., 2010) software was used in this study to process the data. The software works under two main modules. First module is GAMIT and it consists of various programs to process GPS data and results return as the position estimates. The second main module is GLOBK, which is a Kalman filter to combine geodetic solutions from each day.

The data analyses strategy used in this study were as follows:

· Each campaign was processed using the International Terrestrial Reference Frame ITRF-2005 (Altamimi et al., 2007).

· Precise final orbits by the International Global Navigation Satellite Systems (GNSS) Service (IGS) were obtained in SP3 (Standard Product 3) format from SOPAC (Scripps Orbit and Permanent Array Center).

· Earth rotation parameters (ERP) came from USNO_bull_b (United States Naval Observatory_bulletin_b).

· 15 stations from IGS global monitoring network were included in the process. These IGS stations are TUBI,

TRAB, ORID, ANKR, BUCU, ISTA, GRAZ, KIT3, MATE, NICO, NSSP, ONSA, SOFI, WTZR, ZECK.

· The 9-parameter Berne model was used for the effects of radiation and the pressure (Springer et al., 1999).

· IERS conventions for solid earth tide and ocean tide loading effects were adopted (Scherneck, 1991).

· Zenith Delay unknowns were computed based on the Saastamoinen a priori standard troposphere model with 2-h intervals (Saastamonien, 1973).

· Iono-free LC (L3) linear combination of L1 and L2 carrier phases was used.

· Loosely constrained daily solutions obtained from GAMIT were included in the ITRF-2005 reference frame by 7 parameters (3 offset-3 rotation-1 scale) transformation with 15 global IGS stations.

· Geodetic velocities are obtained by applying Kalman filtering method to the results of GPS campaigns. Horizontal GPS velocities are plotted with 95 percent confidence ellipses in Eurasia-fixed frame and shown in Figure 4, and listed in Table 1 (Havazli E., 2012).

The final velocity field estimates that the velocities on and around the Tuzla Fault exceed 20 mm/year which is in agreement with the previous studies regional (McClusky
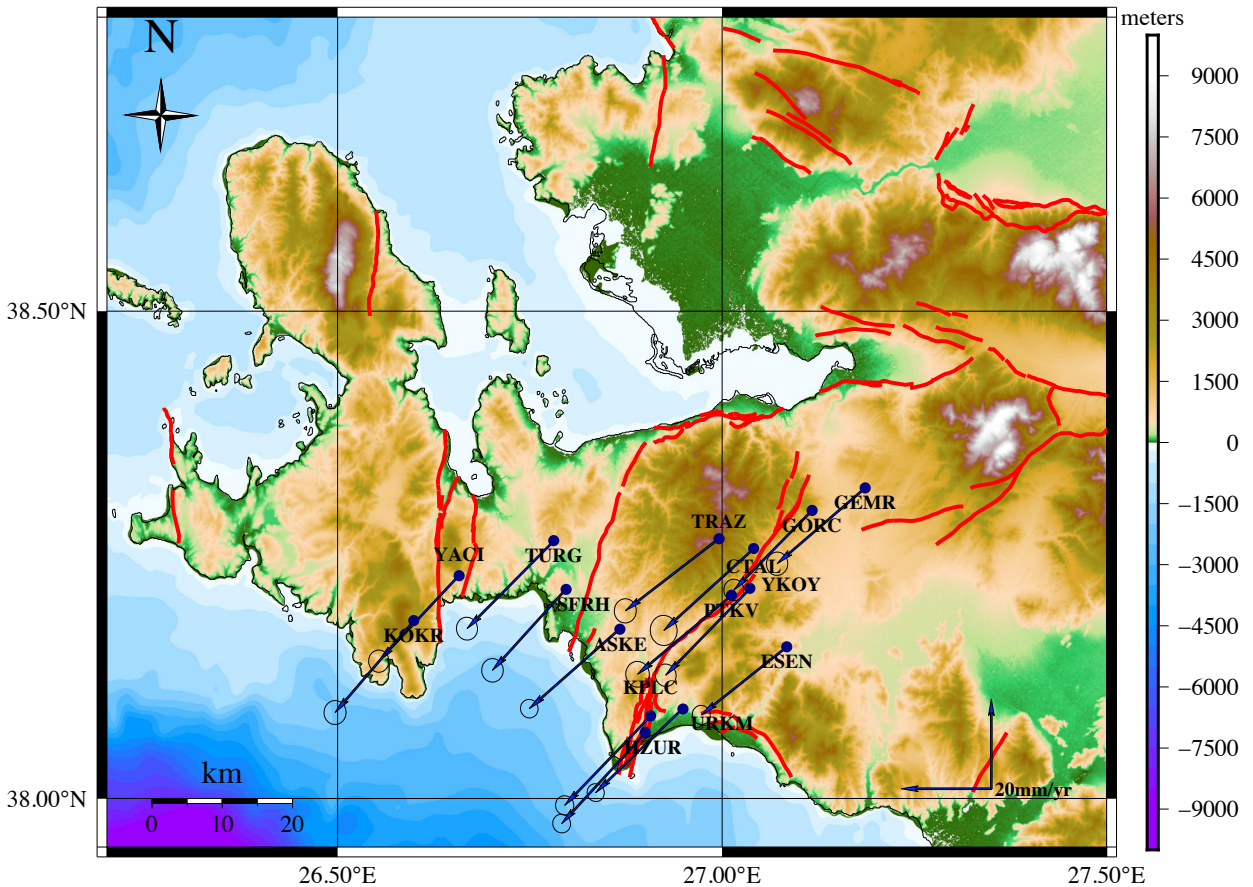

Figure 4. Horizontal velocity field of the study area in Eurasia fixed frame plotted with 95% confidence ellipses.

et al., 2000, Aktug et al., 2009) and local (Ozener et al., 2013) studies. It is expected to achieve the same velocity field with the velocity field given in Ozener et al., 2013, since the input data set and processing standards are the same.

4. Determination of strain accumulation
Two different methods were used to estimate strain rates around the fault. In the first method, the geodetic network was divided into triangles with the corners located at the GPS sites (Table 2). Triangles were chosen to be roughly equilateral and to spatially cover the fault (Havazli, 2012).

Two strain tensors and one azimuth parameters are calculated on each side of the triangle using north and east velocity components of the GPS stations on the corners (Figure 5). We assumed that strain does not vary inside the triangle. Finally, after computation of strain tensor parameters, maximum and minimum principal strain rate components were calculated (Table 3).

Our second approach to estimating strain rates adopts the method developed by Haines and Holt (1993) and updated by Haines et al. (1998) and Beaven and Haines (2001). A bicubic Bessel interpolation was used to expand a model rotation vector function that is obtained by a least-squares minimization for the best fit between the model and observed geodetic velocities. Station velocities are used as input into a strain rate model to calculate strain rates. A technique called spline interpolation is applied by fitting model velocities to observe GPS velocities to define a continuous velocity gradient. The continuous velocity gradient field allows defining strain rate tensor over the study area implicitly. We calculate strain rates on regular 0.5° × 0.5° size grids and then interpolate to correspond to GPS stations (Figure 6). The numerical results of this analysis are given in Table 4.

The main difference between these two methods is their assumption of strain distribution. The method

relying on GPS station velocities on the corners of triangles assume that the strain is homogenously distributed within the triangle, while the method described by Haines and Holt (1993) assume that the strain can be successfully interpolated between GPS stations on an equally spaced grid similar using a bicubic interpolation method. The strength of the first method is that it allows us to estimate strain rates within an area whose sides are constrained by GPS velocities. However, this method cannot be expanded in to larger regions divided by great distances between GPS stations since the assumption of homogenous strain distribution is only true in relatively small areas. This method is particularly helpful in areas with complex fault systems, such as the Aegean region. The second method, which relies on a bicubic interpolation on a regular gird, gives us a chance to calculate strain on any given point within our grid. This method is immensely helpful in regional studies that focus on large areas and connects sparsely or irregularly distributed GPS networks. However, this method's main weakness lies in the assumption of bicubic behavior of strain rates between the grid nodes.

For the purpose of our study, we use the first method to take advantage of its strength in small regions and ability to resolve complex fault systems using velocities from individual GPS stations. We use the second method to take advantage of the ability to estimate strain rates over our GPS stations. Strain rates estimated from both methods represent different aspects of the deformation characteristics on and around the Tuzla Fault.

5. Results and discussion
Results of triangulation method shows that the strain rate over the study are reaches up to 200×10⁻⁹ strain/year, while the results obtained by interpolation method indicates that the strain rates are somewhat lower, reaching 140×10⁻⁹ strain/year over GPS stations. The difference between strain rates should be attributed to the differences between the methods we discussed earlier. It is important to note that the triangulation method is carried out on a subset of the GPS stations we used in this study and, therefore, is limited with the velocities of the chosen subset. This method shows that, where we have a complex fault system (e.g., triangle 2, triangle 6), the magnitude and direction of strain rates differ from triangles with less complexity (e.g., triangle 3, triangle 5).

The results obtained by the interpolation method shows that the stations to the west (ASKE, KOKR, SFRH, TURG and YACI) are deforming in different directions from the stations to the west, which suggests a different deformation regime, influenced by another source other than the Tuzla Fault. We can see that the strain rates calculated over stations HZUR, KPLC, URKMZ are very small, which indicates that they are in a uniform deformation regime

Table 2. Triangle numbers and the GPS stations stations corresponding to the corners of each triangle. The triangles are formed to calculate the strain rate by using velocities of GPS stations on each corner.

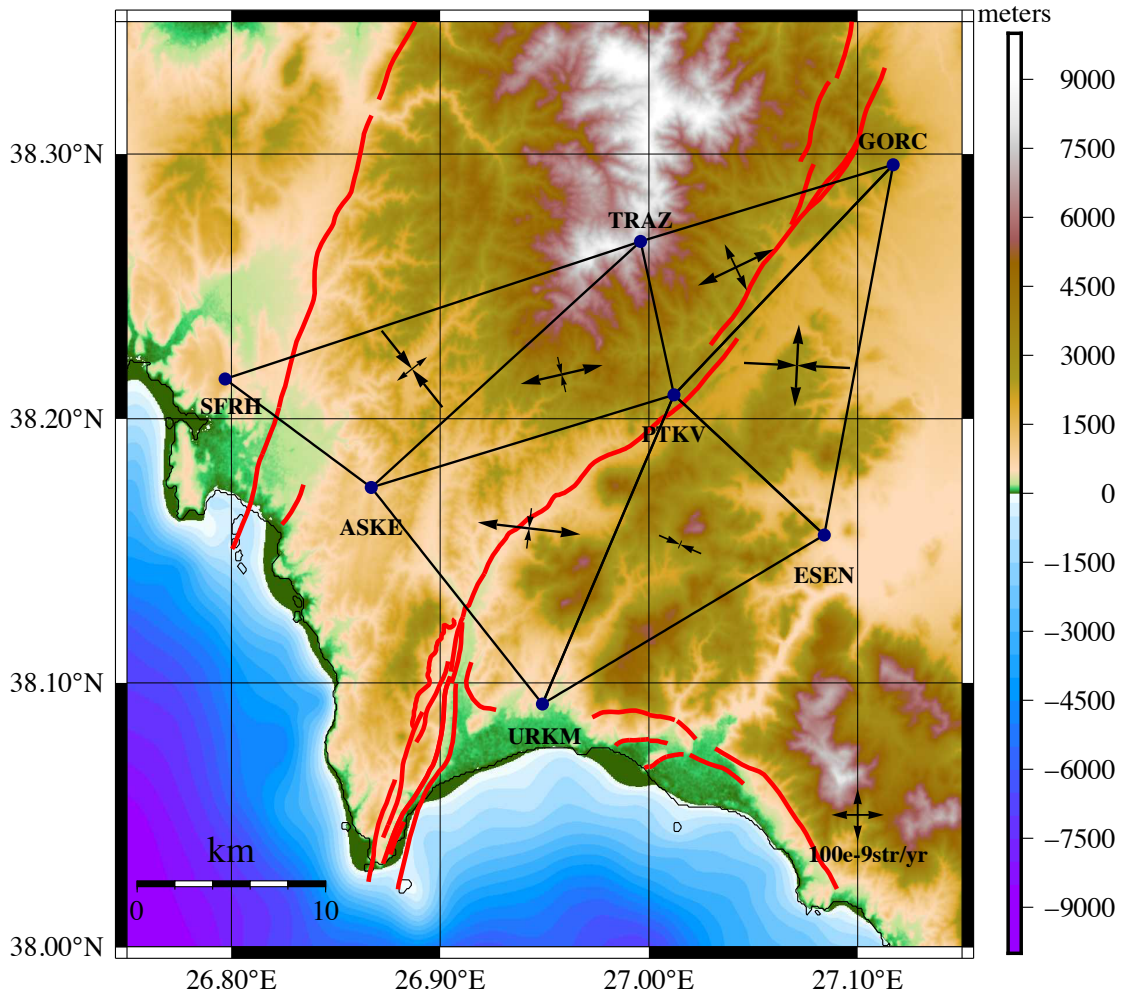| Regions	Site Names
Triangle 1	GORC-ESEN-PTKV
Triangle 2	GORC-PTKV-TRAZ
Triangle 3	ESEN-URKM-PTKV
Triangle 4	URKM-ASKE-PTKV
Triangle 5	PTKV-TRAZ-ASKE
Triangle 6	TRAZ-ASKE-SFRH

Figure 5. Horizontal strain rate field calculation based on triangulation method.

Table 3. Principal strain rates calculated by using the triangulation method. Given locations correspond to the center of the triangles where the principal strain rates are calculated.

Triangle	Latitude (deg)	Longitude (deg)	ε_1 (10⁻⁹/year)	ε_2 (10⁻⁹/year)	Azimuth (deg)
1	38.2201	27.0709	156.39	−201.50	272.7601
2	38.2572	27.0416	160.06	97.72	334.3257
3	38.1524	27.0149	18.97	−87.14	293.4834
4	38.1585	26.9426	196.38	−77.50	6.6481
5	38.2167	26.9582	160.11	−68.92	347.0351
6	38.2188	26.8865	73.27	−185.62	321.5866

and, therefore, accumulating minimum strain while actively deforming.

Strain rate values and direction of extension and compression from both methods are consistent with present day kinematics of the Aegean region reported in previous studies (e.g., Aktug and Kılıçoğlu, 2006). Our results indicate that the strain rate increases from west to east, which may indicate a higher risk of a large earthquake closer to the city of İzmir. The abundance of small, active faults in the region supports the idea claiming that the
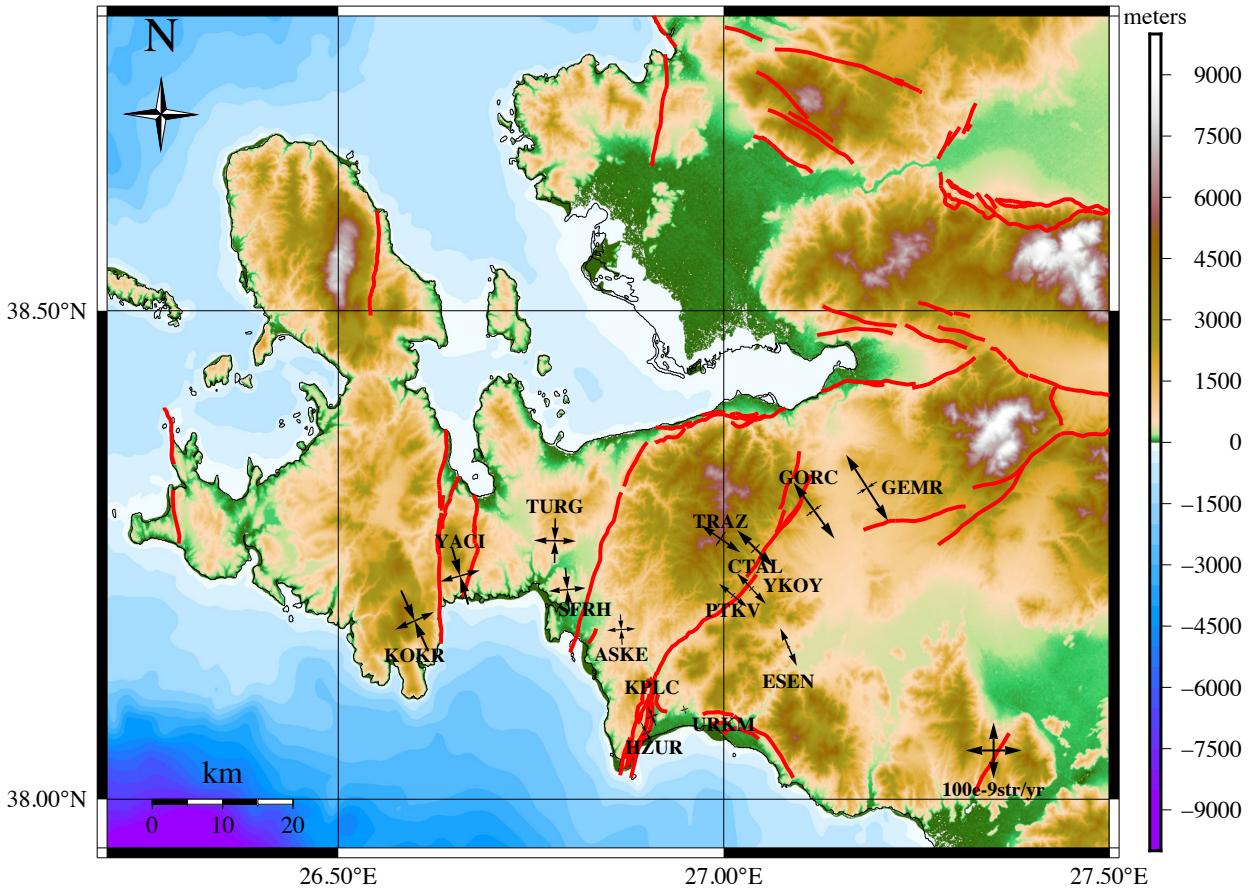
Figure 6. Horizontal strain rate field calculation based on the algorithm of Holt and Haines (1993&1998).

Table 4. Principal strain rates calculated by using the interpolation method described in Holt and Haines (1993).

Site	Latitude (deg)	Longitude (deg)	ε_1 (10^{-9}/year)	ε_2 (10^{-9}/year)	Azimuth (deg)
ESEN	38.156	27.084	−6.065	73.34	66.3879
CTAL	38.257	27.041	−21.32	92.07	45.3361
YKOY	38.216	27.036	−11.26	74.66	46.8435
PTKV	38.209	27.012	−11.24	64.05	39.6234
TRAZ	38.267	26.996	−29.59	84.98	34.7658
URKM	38.092	26.949	−14.41	16.02	161.2142
KPLC	38.085	26.907	−36.51	23.57	157.3640
HZUR	38.068	26.900	−41.54	22.44	151.7589
ASKE	38.174	26.867	−54.06	50.31	176.6960
SFRH	38.215	26.797	−78.22	65.70	175.1389
TURG	38.265	26.781	−79.41	74.51	1.0495
YACI	38.229	26.658	−105.91	72.65	164.1452
KOKR	38.183	26.599	−118.57	75.60	155.9078
GEMR	38.319	27.186	−40.81	139.26	57.6269
GORC	38.296	27.117	−32.37	123.68	53.9733

difference is caused by another actively deforming fault located to the west and not yet known or mapped. For this reason, to better understand the complex deformation regime of the study area, further investigations are required.

6. Conclusion

Main findings of our study are: The Tuzla Fault is accumulating stress and strain with an increasing rate from west to east that may pose a threat to the city of İzmir; the different methods used to estimate strain rates are complementary, and they tell us that there are multiple fault systems actively deforming in the area.

Our findings are in agreement with the previous regional studies which indicates that long term deformation is continuous in the study area.

References

Aktuğ B, Kılıçoğlu A (2006). Recent crustal deformation of İzmir, Western Anatolia and surrounding regions as deduced from repeated GPS measurements and strain field. Journal of Geodynamics 41 (5): 471-484. doi: 10.1016/j.jog.2006.01.004

Aktug B, Nocquet JM, Cingöz A, Parsons B, Erkan Y et al. (2009). Deformation of western Turkey from a combination of permanent and campaign GPS data: Limits to block-like behavior. Journal of Geophysical Research 114 (B10). doi: 10.1029/2008jb006000

Altamimi Z, Sillard P, Boucher C (2002). ITRF2000: A new release of the International Terrestrial Reference Frame for earth science applications. Journal of Geophysical Research: Solid Earth 107 (B10): ETG 2–1–ETG 2–19. doi: 10.1029/2001jb000561

Altamimi Z, Collilieux X, Legrand J, Garayt B, Boucher C (2007). ITRF2005: A new release of the International Terrestrial Reference Frame based on time series of station positions and Earth Orientation Parameters. Journal of Geophysical Research 112 (B9). doi: 10.1029/2007jb004949

Armijo R, Meyer B, King GCP, Rigo A, Papanastassiou D (1996). Quaternary evolution of the Corinth Rift and its implications for the Late Cenozoic evolution of the Aegean. Geophysical Journal International 126 (1): 11-53. doi: 10.1111/j.1365 246x.1996.tb05264.x

Beavan J, Haines J (2001). Contemporary horizontal velocity and strain rate fields of the Pacific-Australian plate boundary zone through New Zealand. Journal of Geophysical Research: Solid Earth 106 (B1): 741-770. doi: 10.1029/2000jb900302

Danciu L, Şeşetyan K, Demircioğlu M, Gülen L, Zare M et al. (2018). The 2014 earthquake model of the Middle East: seismogenic sources. Bulletin of Earthquake Engineering 16 (8): 3465-3496. doi: 10.1007/s10518-017-0096-8.

Emre Ö, Barka A (2000). Active faults between Gediz Graben and Aegean Sea (İzmir region). In: Proceedings of Seismicity of western Anatolia Symposium. Dokuz Eylül University Publications: 131-132. (in Turkish with English abstract)

Emre O, Ozalp S, Dogaz A, Ozaksoy V, Yildirim C et al. (2005). The report on faults of Izmir and its vicinity and their earthquake potentials. General Directorate of Mineral Research and Exploration Report: (10754). (in Turkish)

Ergun M, Oral EZ (2000). General tectonic elements of the Eastern Mediterranean and implications. In: Proceedings of International Symposia on Seismicity of Western Anatolia.

Esder T, Caglav F, Pekatan R, Yakabag A (1988). The Feasibility Report for the Area and the Geothermal Wellhole Of Cumali-Tuzla (Seferihisar-Izmir): No. 8146. GDMRE Report. (in Turkish)

Genç CŞ, Altunkaynak Ş, Karacık Z, Yazman M, Yılmaz Y (2001). The Çubukludağ graben, south of İzmir: its tectonic significance in the Neogene geological evolution of the western Anatolia. Geodinamica Acta 14 (1-3): 45-55. doi: 10.1080/09853111.2001.11432434

Haines AJ, Holt WE (1993). A procedure for obtaining the complete horizontal motions within zones of distributed deformation from the inversion of strain rate data. Journal of Geophysical Research: Solid Earth 98 (B7): 12057-12082. doi: 10.1029/93jb00892

Haines AJ, Jackson JA, Holt WE, Agnew DC (1998). Representing Distributed Deformation by Continuous Velocity Fields, Rep. 98/5. Lower Hutt, New Zealand: Institute of Geological and Nuclear Sciences.

Halicioglu K, Ozener H (2008). Geodetic network design and optimization on the active Tuzla Fault (İzmir, Turkey) for disaster management. Sensors 8 (8): 4742-4757. doi: 10.3390/s8084742

Havazli E, (2012). Determination of strain accumulation along Tuzla Fault, MSc., Boğazici University, Kandilli Observatory and Earthquake Research Institute, Geodesy Department, İstanbul, Turkey.

Herring TA, King RW, McClusky SC (2010). Introduction to GAMIT/GLOBK. Cambridge, MA, USA: Massachusetts Institute of Technology.

Holt WE, Haines AJ (1995). The kinematics of northern South Island, New Zealand, determined from geologic strain rates. Journal of Geophysical Research: Solid Earth 100 (B9): 17991-18010. doi: 10.1029/95jb01059

Ilhan T, Utku M, Ozyal N, Utku Z (2004). Earthquake risk of Izmir region. İzmir, Turkey: Dokuz Eylül University Marine Science Institute Press.

Jackson JA, Gagnepain J, Houseman G, King GCP, Papadimitriou P et al. (1982). Seismicity, normal faulting, and the geomorphological development of the Gulf of Corinth (Greece): the Corinth earthquakes of February and March 1981. Earth and Planetary Science Letters 57 (2): 377-397. doi: 10.1016/0012-821x(82)90158-3

Jackson J, McKenzie D (1988). The relationship between plate motions and seismic moment tensors, and the rates of active deformation in the Mediterranean and Middle East. Geophysical Journal International 93 (1): 45-73. doi: 10.1111/j.1365-246x.1988.tb01387.x

Kandilli Observatory and Earthquake Research Institute, Boğaziçi University (1971). Boğazici University Kandilli Observatory and Earthquake Research Institute [Data set]. International Federation of Digital Seismograph Networks. doi: 10.7914/SN/KO

Koçyiğit A (2000). Seismicity of Southwestern Turkey. In: Proceedings of International Symposia on Seismicity of Western Anatolia, Izmir, Turkey.

Kreemer C, Holt WE, Goes S, Govers R (2000). Active deformation in eastern Indonesia and the Philippines from GPS and seismicity data. Journal of Geophysical Research: Solid Earth, 105 (B1): 663-680. doi:10.1029/1999jb900356

McKenzie D (1972). Active tectonics of the Mediterranean Region. Geophysical Journal International 30 (2): 109-185. doi: 10.1111/j.1365-246x.1972.tb02351.x

McKenzie, D. (1978). Active tectonics of the Alpine--Himalayan belt: the Aegean Sea and surrounding regions. Geophysical Journal International 55 (1): 217-254. doi: 10.1111/j.1365-246x.1978.tb04759.x

McClusky S, Balassanian S, Barka A, Demir C, Ergintav S et al. (2000). Global Positioning System constraints on plate kinematics and dynamics in the eastern Mediterranean and Caucasus. Journal of Geophysical Research: Solid Earth 105 (B3): 5695–5719. doi: 10.1029/1999jb900351

Mercier JL, Sorel D, Vergely P, Simeakis K (1989). Extensional tectonic regimes in the Aegean basins during the Cenozoic. Basin Research 2 (1): 49-71. doi: 10.1111/j.1365-2117.1989.tb00026.x

Mueller S, Kahle HG, Barka A (1997). Plate tectonic situation in the Anatolian-Aegean region. Active tectonics of Northwestern Anatolia-The Marmara Polyproject. Zürich, Switzerland: VDF, Hoschschulverlag AG an der ETH, pp. 13-28.

Nyst M, Thatcher W (2004). New constraints on the active tectonic deformation of the Aegean. Journal of Geophysical Research: Solid Earth 109 (B11): doi: 10.1029/2003jb002830

Ocakoğlu N, Demirbağ E, Kuşçu İ (2005). Neotectonic structures in İzmir Gulf and surrounding regions (western Turkey): Evidences of strike-slip faulting with compression in the Aegean extensional regime. Marine Geology 219 (2-3): 155-171. doi: 10.1016/j.margeo.2005.06.004

Ozener H, Dogru A, Acar M (2013). Determination of the displacements along the Tuzla fault (Aegean region-Turkey): Preliminary results from GPS and precise leveling techniques. Journal of Geodynamics 67: 13-20. doi: 10.1016/j.jog.2012.06.001

Paton S (1992). Active normal faulting, drainage patterns and sedimentation in southwestern Turkey. Journal of the Geological Society 149 (6): 1031-1044. doi: 10.1144/gsjgs.149.6.1031

Piper J, Gursoy H, Tatar O (2001, May). Palaemagnetic analysis of Neotectonic Crustal Deformation in Turkey. In: Proceeding of Symposia on Seismotectonics of the North-Western Anatolia-Aegean and Recent Turkish Earthquakes (Vol. 8).

RADIUS (1997). Risk Assessment Tools For Diagnosis Of Urban Areas Against Seismic Disaster İzmir Earthquake Master Program. İstanbul, Turkey: Bogazici University Kandilli Observatory.

Reilinger R, McClusky S (2011). Nubia-Arabia-Eurasia plate motions and the dynamics of Mediterranean and Middle East tectonics. Geophysical Journal International 186 (3): 971-979. doi: 10.1111/j.1365-246x.2011.05133.x

Saastamoinen J (1973). Contributions to the theory of atmospheric refraction. Bulletin Géodésique 107 (1): 13-34. doi: 10.1007/bf02522083

Sabuncu A, Ozener H (2013). Monitoring vertical displacements by precise levelling: a case study along the Tuzla Fault, Izmir, Turkey. Geomatics, Natural Hazards and Risk 5 (4): 320-333. doi: 10.1080/19475705.2013.810179

Saroglu F, Emre O, Boray A (1987). Türkiye'nin Diri Fayları ve Depremselliği, MTA, Report No: 8174. (in Turkish)

Saroglu F, Emre O, Kuşçu İ (1992). Türkiye Diri Fay Haritası, 1:2,000,000 ölçekli, Maden Tetkik ve Arama Genel Müdürlügü, Ankara.

Saunders P, Priestley K, Taymaz T (1998). Variations in the crustal structure beneath western Turkey. Geophysical Journal International 134 (2): 373-389. doi: 10.1046/j.1365-246x.1998.00571.x

Scherneck HG (1991). A parametrized solid earth tide model and ocean tide loading effects for global geodetic baseline measurements. Geophysical Journal International 106 (3): 677-694. doi: 10.1111/j.1365-246x.1991.tb06339.x

Şengör AMC, Yılmaz Y (1981). Tethyan evolution of Turkey: A plate tectonic approach. Tectonophysics 75 (3-4): 181-241. doi: 10.1016/0040-1951(81)90275-4

Sodoudi F, Kind R, Hatzfeld D, Priestley K, Hanka W et al. (2006). Lithospheric structure of the Aegean obtained from P and S receiver functions. Journal of Geophysical Research: Solid Earth 111 (B12). doi: 10.1029/2005jb003932

Shen-Tu B, Holt WE, Haines AJ (1999). Deformation kinematics in the western United States determined from Quaternary fault slip rates and recent geodetic data. Journal of Geophysical Research: Solid Earth 104 (B12): 28927-28955. doi: 10.1029/1999jb900293

Springer TA, Beutler G, Rothacher M (1999). A new solar radiation pressure model for GPS satellites. GPS Solutions 2 (3): 50-62. doi: 10.1016/S0273-1177(99)00158-1

Tan O, Taymaz T (2001). Source parameters of November 6, 1992 Doganbey (Izmir) Earthquake (Mw = 6.0) Obtained from Inversion of Teleseismic Body-Waveforms, 4th International Turkish Geology Symposium, 24–28 September 2001, Cukurova University, Abstract volume, p. 171, Adana.

Taymaz T, Jackson J, McKenzie D (1991). Active tectonics of the north and central Aegean Sea. Geophysical Journal International 106 (2): 433-490. doi: 10.1111/j.1365-246x.1991.tb03906.x

Taymaz T, Yılmaz Y, Dilek Y (2007). The geodynamics of the Aegean and Anatolia: introduction. Geological Society, London, Special Publications, 291 (1): 1-16. doi: 10.1144/sp291.1

Utku M (2000). Position of Western Anatolia in Turkey's seismicity. In: Proceedings of the Symposium of the Western Anatolia seismicity (pp. 24-27).

Wessel P, Luis JF, Uieda L, Scharroo R, Wobbe F et al. (2019). The generic mapping tools version 6. Geochemistry, Geophysics, Geosystems 20: 5556-5564. doi: 10.1029/2019GC008515

Yılmaz Y (2000, May). Active tectonics of Aegean region. In: Proceedings of International Symposia on Seismicity of Western Anatolia (pp. 24-27).